BBA - General Subjects xxx (xxxx) xxx–xxx

Contents lists available at ScienceDirect

BBA - General Subjects

journal homepage: www.elsevier.com/locate/bbagen

Helicobacter pylori antigenic Lpp20 is a structural homologue of Tipα and promotes epithelial-mesenchymal transition

Francesca Vallese[a,1], Nigam M. Mishra[a,1,2], Matteo Pagliari[b], Paola Berto[a], Gaia Codolo[b], Marina de Bernard[b,*], Giuseppe Zanotti[a,*]

[a] Department of Biomedical Sciences, University of Padua, Via Ugo Bassi 58/B, Padua 35131, Italy
[b] Department of Biology, University of Padua, Via Ugo Bassi 58/B, Padua 35131, Italy

ARTICLE INFO

Keywords:
Helicobacter pylori
Crystal structure
Lipoprotein
Epithelial–mesenchymal transition

ABSTRACT

Background: *Helicobacter pylori* is a bacterium that affects about 50% of the world population and, despite being often asymptomatic, it is responsible of several gastric diseases, from gastritis to gastric cancer. The protein Lpp20 (HP1456) plays an important role in bacterium survival and host colonization, but the possibility that it might be involved in the etiology of *H. pylori*-related disorders is an unexplored issue. Lpp20 is a lipoprotein bound to the external membrane of the bacterium, but it is also secreted inside vesicles along with other two proteins of the same operon, i.e. HP1454 and HP1457.

Results: In this study we determined the crystal structure of Lpp20 and we found that it has a fold similar to a carcinogenic factor released by *H. pylori*, namely Tipα. We demonstrate that Lpp20 promotes cell migration and E-cadherin down-regulation in gastric cancer cells, two events recalling the epithelial–mesenchymal transition (EMT) process. Differently from Tipα, Lpp20 also stimulates cell proliferation.

Conclusions: This identifies Lpp20 as a new pathogenic factor produced by *H. pylori* that promotes EMT and thereby the progression of cancer to the metastatic state.

1. Introduction

Helicobacter pylori is a bacterium that infects about 50% of the world population and, despite being often asymptomatic, it is responsible for several gastric diseases, from gastritis to gastric cancer [1] [2].

The development of a vaccine has been sought for long time [3], and several proteins have been discovered to be antigenic and eventually proposed to become components of a vaccine: they include the urease enzyme [4] and its chaperonin [5], the cytotoxin VacA [6], the catalase [7], the Neutrophil Activating Protein HP-NAP [8–11], and various outer-membrane or membrane-associated proteins [12]. Quite recently, an oral vaccine against the subunit B of urease fused with the B subunit of the *E. coli* heath-labile enterotoxin has entered phase 3 clinical trial [13]. Among the possible vaccine candidates, a protein called Lpp20, corresponding to the product of gene *hp1456*, has been considered [14], since it was identified as one of the major antigens recognized by sera of *H. pylori*-infected subjects. Moreover, guinea pigs immunized with a chimeric protein of Lpp20 and interleukin 2 induced strong cellular immunity in mice [15], and a vaccine composed by three Lpp20-derived epitopes and the cholera toxin B subunit was constructed and tested in mice [16].

Despite the physiological role of Lpp20 for the bacterium is not known, odd are it plays an important role in its survival, since it is up-regulated by an environmental acidic pH [17] and by iron depletion [18] [19]. Furthermore, even if an isogenic mutant defective in the production of Lpp20 apparently displayed normal viability, [20], *hp1456* was confirmed as one of the 344 genes essential for bacterium survival [21]. Lpp20 is located in the cell envelope but it is also released inside membrane vesicles in the culture medium [22]. It is a protein of 175 amino acids, with a molecular weight of about 19,000 Da that contains a signal peptide sequence of 21 amino acids at the N-terminus. The mature protein is composed of 154 amino acids for a molecular weight of 18,283 Da [20]. Lpp20 is predicted to be lipidated by N-palmitoyl or S-diacylglycerol at cysteine 22, the first amino acid after

Abbreviations: r.m.s.d., root mean square deviation; EMT, epithelial–mesenchymal transition; DTT, dithiothreitol

* Corresponding author.
E-mail addresses: marina.debernard@unipd.it (M. de Bernard), giuseppe.zanotti@unipd.it (G. Zanotti).
URL: http://tiresia.bio.unipd.it/zanotti (G. Zanotti).

[1] Equal contribution.

[2] Present address: System College of Pharmacy, Department of Pharmaceutical Sciences, University of North Texas Health Science Center, 3500 Camp Bowie Boulevard, Fort Worth 76107, Texas, USA.

http://dx.doi.org/10.1016/j.bbagen.2017.09.017
Received 4 August 2017; Received in revised form 7 September 2017; Accepted 21 September 2017

the processing of the protein by a lipoprotein signal peptidase.

With the aim of verifying whether Lpp20 could have a role in the pathogenesis of *H. pylori*-related disorders, we determined the three-dimensional structure of the protein and sought for structural homologies with known virulence factors. We found that Lpp20 shares the same architecture with Tipα, a carcinogenic factor produced by *H. pylori* that induces TNF-α and chemokine gene expression by activating NF-κB [23,24]. Tipα is considered an inducer of the epithelial–mesenchymal transition (EMT), a process by which epithelial cells lose their cell polarity and cell-cell adhesion, and gain migratory and invasive properties to become mesenchymal stem cells [25] [26]. EMT has also been shown to occur in the initiation of metastasis for cancer progression. By taking advantage of a recombinant form of Lpp20, we demonstrated that Lpp20 promotes cell migration and E-cadherin down-regulation in gastric cancer cells, and that it stimulates cell proliferation. This identifies Lpp20 as a new pathogenic factor produced by *H. pylori*.

2. Materials and methods

2.1. Molecular cloning

The coding sequence of HP1456 (Δ1–21) gene was amplified from genomic *H. pylori* DNA (strain 26695) using the primers 5′-CATCATCACCACCATCAC.

GAAAACCTGTATTTCCAGGGTGCTGCTTGCAGCCATGCCCCAAAA-3′ (forward) and 5′-GTGGCGGCCGCTCTATTACTTTTTAACCATGCCCAA-3′ (reverse). The gene was cloned into pETite vector suitable for T7-driven expression in *E. coli* (Lucigen, UK), in frame with an N-terminal His-tag and flanked by a TEV cleavage site. Lpp20 mutant in cysteine 22 (lpp20C22A) was obtained with the QuikChange II Site-Directed Mutagenesis Kit (Agilent, CA) from the pETite-lpp20 plasmid, using the primers 5′–TTCCAGGGTGCTGCTGCCAGCCATGCCCCAAAA-3′ (forward) and 5′–TTTTGGGGCATGGCTGGCAGCAGCACCCTGGAA-3′ (reverse).

2.2. Protein expression and purification

E. coli BL21(DE3)-pLysS competent cells were transformed with the recombinant plasmid, and positive clones were selected according to kanamicin resistance (30 $\mu g \cdot ml^{-1}$). A 2-l culture was obtained starting from an overnight pre-culture of transformed cells. Cells were grown at 37 °C until the $OD_{600\ nm}$ reached the value of 0.5. Expression was induced by adding 1 mM isopropyl-b-D-thiogalactopyranoside (IPTG) to the LB medium and the growth was prolonged for 4 h at 37 °C under constant shaking. Bacterial pellet was harvested by centrifugation (6000 × *g* for 20 min), resuspended in lysis buffer (20 mM Tris-HCl, pH 7.4, 200 mM NaCl plus 1 mM PMSF), and lysed using a One-Shot Cell disruption system (Constant Systems Ltd) operated at 1.35 kbar. Lysate was centrifuged at 14000 × *g* for 20 min at 4 °C to separate supernatant from cell debris. The soluble fraction was incubated with a His-select Nickel affinity gel (Sigma Aldrich) at 4 °C for 2 h. After incubation, the resin was extensively washed with wash buffer (20 mM Tris-HCl, pH 7.4, 150 mM NaCl and 20 mM imidazole). Lpp20 was eluted with elution buffer (20 mM Tris-HCl, pH 7.4, 150 mM NaCl and 500 mM imidazole). To prevent protein precipitation, imidazole was removed using PD-10 desalting column (GE Healthcare) equilibrated with a buffer consisting of 50 mM Tris-HCl, pH 7.4, 150 mM NaCl. Concentrated sample was further purified using FPLC. Gel filtration was performed on a Superose 12 10/300 GL size-exclusion column, equilibrated in a buffer containing 50 mM Tris-HCl, pH 7.4, 150 mM NaCl. Lpp20 eluted as two peaks, one corresponding to the monomer and the other to the dimeric form of the protein. The two peaks were collected separately, and concentrated to 16 mg/ml.

For Se-Met incorporation into Lpp20, *E. coli* cells were grown in minimal medium M9 supplemented with 0.4% (w/v) glucose, salts, and all the amino acids except Met, substituted by Se-Met. Approximately 30 min before induction with IPTG, a solution of Se-Met plus Leu, Ile, Val, Phe, Lys, and Thr was added to the medium to inhibit the *E. coli* methionine pathway and to force the incorporation of Se-Met. The Lpp20 Se-Met derivative was purified analogously to that described for the native protein. Lpp20C22A protein was purified as described for Lpp20 wild type.

2.3. Interaction with HP1454, HP1455 and HP1457

HP1454 was expressed and purified as described [27]. HP1455 and HP1457 were cloned in pETite vector and purified with nickel affinity chromatography. All three proteins have the histidine tag. To determine the possible interaction between Lpp20 and these proteins, the His-tag of Lpp20 protein was removed. For this purpose, purified Lpp20 was incubated overnight at 4 °C with TEV Protease (Sigma) and once the protein without the tag was recovered, it was incubated separately with each of the other proteins. The removal of the tag from Lpp20 was checked by western blot using an Anti-polyHistidine antibody (Sigma, Germany) and the inability of the cleaved Lpp20 to bind to the nickel resin was verified. After an incubation at 4 °C for 2 h, the couples of proteins were again subjected to an affinity chromatography taking advantage of the His-tag of the interacting partners. Co-elution was verified by SDS-PAGE.

2.4. Crystallization and data collection

Purified Lpp20 was concentrated to 16 mg/ml and used for crystallization trials, partially automated by an Oryx 8 crystallization robot (Douglas Instruments, UK). The protein crystallized in several different conditions of the PEGS-II Suit screen (Quiagen, Germany). The best crystals were obtained at 20 °C by vapor diffusion using as precipitant a solution containing 0.2 M $CaCl_2$, 0.1 M HEPES (pH 7.5), 20% PEG 6000 (solution number 44 of PEGS-II Suit screen, Quiagen, Germany). In order to solve the phase problem, Se-Met derivatized Lpp20 crystals were prepared. Se-Met derivatives crystals successfully grew in the same conditions of native protein.

Native diffraction data were measured at the PXIII beamline at the Swiss Synchrotron Light Source (SLS, Villigen, Switzerland), and Se-Met derivatives at the ID23-2 beamline of the European Synchrotron Radiation Facility (ESRF, Grenoble, France). Crystals were flash frozen at 100 K before data collection. Crystals of both native and Se-Met derivatives belong to the orthorhombic space group $P2_12_12_1$. Cell dimensions of the native crystal used for the final refinement are **a** = 55.303 Å, **b** = 90.424 Å, **c** = 114.522 Å (Table 1). Four monomers are present in the asymmetric unit, corresponding to a V_M of 2.83 $Å^3$/Da and an approximate solvent content of 56%. All diffraction data were indexed, integrated with software XDS [28], merged and scaled with software Scala [29], contained in the CCP4 crystallographic package [30]. The SAD data allowed to obtain an initial density map using software Autosol [31]. Initial phases were submitted to the *Buccaneer* software [32] for density modifications and model building. The model obtained was used for refinement against the native data-set at higher resolution with Phenix [33] and checked, as well as manually adjusted, with the graphic software Coot [34]. Solvent molecules were added automatically by the program and checked manually. One HEPES molecule and one Ca^{2+} ion are present in between monomers B, C and D in the crystal. The final statistics on data collection and refinement are summarized in Table 1.

2.5. Cell culture

Two human gastric cancer cell lines were used: AGS (poorly differentiated gastric adenocarcinoma) and MKN-28 (well differentiated gastric adenocarcinoma). Both cell lines were grown in RPMI 1640 medium (Euroclone) with 10% fetal bovine serum (FBS), 1 mM HEPES (Gibco, Thermo Fisher Scientific) and penicillin-streptomycin

Table 1
Statistics of data collection, processing and refinement. Values for the outer shell are given in parentheses. 1800 frames of 0.1° oscillation were collected.

	Native	Se-MET derivative SAD data
Space group	$P2_12_12_1$	$P2_12_12_1$
Wavelength (Å)	1.00002	0.97897
Unit cell parameters (Å, °)	a = 55.303	a = 54.260
	b = 90.424	b = 89.016
	c = 114.522	c = 114.180
Resolution range (Å)	48.38–1.86 (1.97–1.86)	49.01–2.08 (2.15–2.08)
Independent reflections	46,285	33,876
R_{merge}	0.040 (0.992)	0.085 (1.339)
R_{pim}	0.018 (0.471)	0.039 (0.588)
$\langle I/\sigma(I)\rangle$	21.0 (1.6)	14.0 (1.3)
Completeness (%)	98.5 (89.9)	99.5 (95.1)
Anomalous completeness (%)		98.9 (92.2)
Redundancy	6.5 (6.1)	71. (6.9)
Refinement		
R_{work}/R_{free}	0.229/0.268	
No. protein/solvent atoms/ligands	3563/367/16	
Mean B (Å^2)	62.1	
R.m.s.d. from ideal value		
Bond length (Å)	0.0084	
Bond angles (°)	1.03	
Geometry		
Ramachandran favored (%)	99.3	
Ramachandran outliers (%)	1	
Rotamer outliers (%)	1.0	
Overall score	1.45	

antibiotics (Sigma, Germany) at 37 °C under 5% CO_2.

2.6. Western blotting

MKN-28 cells were lysed with lysis buffer containing 20 mM Tris-HCl pH 8.0, 150 mM NaCl, 1% Triton X-100, 1 mM Protease Inhibitor Cocktails (PIC) and PhosSTOP (Roche, Germany). 40 μg of cell lysates were subjected to SDS-PAGE and then transferred onto PVDF membranes (Millipore, US). Membranes were blocked with 5% BSA (Sigma, US) in TBS (50 mM Tris-Cl, pH 7.6; 150 mM NaCl) with 0.1% Tween 20, and then incubated with primary antibodies. Rabbit polyclonal antibody against E-cadherin was purchased from Cell Signaling (Palo Alto, CA) and a monoclonal antibody against β-actin (C4) was purchased from Santa Cruz (Dallas, Texas). Proteins were revealed using rabbit or mouse peroxidase-conjugated secondary antibodies with Enhanced ChemiLuminescence (ECL) system (Millipore, USA).

2.7. Transwell migration assay

Migration assays were performed as previously described [35] using transwell chambers 8 μm size pore (Corning Inc., Corning, NY, USA). Chambers were inserted into a 24-well plate and 2×10^4 AGS cells were plated in 300 μl of serum-free RPMI on the membrane of the upper chamber. Serum-free RPMI (supplemented with 0.1% BSA) was added into the lower chamber of each well together with either Lpp20 or Lpp20C22A recombinant proteins (60 μg/ml). Cells kept unstimulated were considered as negative control. After 24 h, cells on the top of the filter were removed by scrubbing twice with a cotton-tipped swab. Migrated cells (on the bottom of the filter) were fixed in glutaraldehyde 2.5% for 10 min and stained with 0.2% crystal violet for 10 min. Filters were washed with water until the excess of dye was removed. Different fields were randomly selected in each chamber to observe cells. Pictures were taken at 25 × and 80 × magnification. Each experimental group was repeated three times and the number of migrated cells was counted under a microscope.

2.8. Scratch assay

AGS and MKN-28 cells were seeded and grown in 6-well plates at a density of 3×10^4 cells/well until they reached a confluence of ~80%. A scratch was made through each well using a sterile pipette tip. Debris were removed by gentle washing with medium and either Lpp20 or Lpp20C22A recombinant proteins (60 μg/ml) were added. Cells were monitored under the microscope (magnification, 150 ×) at time 0, and after 6 h and 24 h (wounding at 37 °C in 5% CO_2). Images of cells were captured at the same position before and after the treatment to document the repair process. The experiments were repeated three times and representative pictures are shown.

2.9. Staining of actin filaments with phalloidin

5×10^4 AGS and 10^5 MKN-28 cells were seeded in RPMI 1640 10% FBS on coverslips in 24-well plates. Cells were exposed to Lpp20 or Lpp20C22A (60 μg/ml) in serum-free RPMI 1640, 0.1% BSA, or maintained in serum-free RPMI 1640, 0.1% BSA without any stimulation, for 24 h at 37 °C and then washed with PBS. Cells were fixed with 4% paraformaldehyde and permeabilized with 0.3% Triton X-100 in PBS 5 min at RT. After blocking 1 h at RT with 3% goat serum in PBS, cells were stained with TRITC-conjugated phalloidin (Sigma), diluted 1:200 in PBS, 1 h at RT. Nuclei were stained with Hoechst 33,342 (Thermo Fisher). Images were collected with a Leica SP5 confocal microscope equipped with a 63 × HCX PL APO NA 1.4.

2.10. RT-PCR

Total RNA was isolated from cells using TRIzol solution (Thermo Fisher Scientific) according to the manufacturer's instruction. RNA was reverse-transcribed using SuperScript II (Thermo Fisher Scientific), and cDNA was amplified with the following primers:

GAPDH, 5′-AGCAACAGGGTGGTGGAC-3′ and 5′-GTGTGGTGGGGGACTGAG-3′.

E-cadherin, 5′-ACACCATCCTCAGCCAAGA-3′ and 5′-CGTAGGGAAACTCTCTCGGT-3′.

RT-PCR reaction was performed in a 7900HT Fast Real-Time PCR System (Applied Biosystem). After amplification, data analysis was performed using the ΔΔCt method. For each sample, data were normalized to the endogenous reference gene GAPDH and expressed as arbitrary units.

2.11. Proliferation assay

Cell proliferation was determined by dilution of 5-(and −6) carboxyfluorescein diacetate, succinimidyl ester probe (CFDA-SE, Thermo Fisher Scientific). Briefly, AGS cells were resuspended in pre-warmed PBS at the density of 1×10^6/ml and labeled with 2 μM CFDA-SE for 10 min at 37 °C. Cells were then washed with PBS three times to remove unbound CFDA-SE and resuspended in serum-free RPMI 1640. 1.2×10^5 cells were seeded in 24-well plates and treated with Lpp20 or Lpp20C22A (60 μg/ml), or left untreated, in RPMI 1640, 0.1% BSA. After 24 h cells were harvested and the proliferation rate was assessed by flow cytometry (FACSCanto II, BD Bioscience). Data were analyzed with FlowJo software (Treestar).

2.12. Statistical analysis

The results are presented as SEMs of three experiments using AGS or MKN-28 cells. Band intensities were expressed referring to unstimulated cells, set as 1. Data were analyzed by Alliance 1D software and the Student's ***t***-test was performed. The level of significance was $*p < 0.05$, $**p < 0.01$.

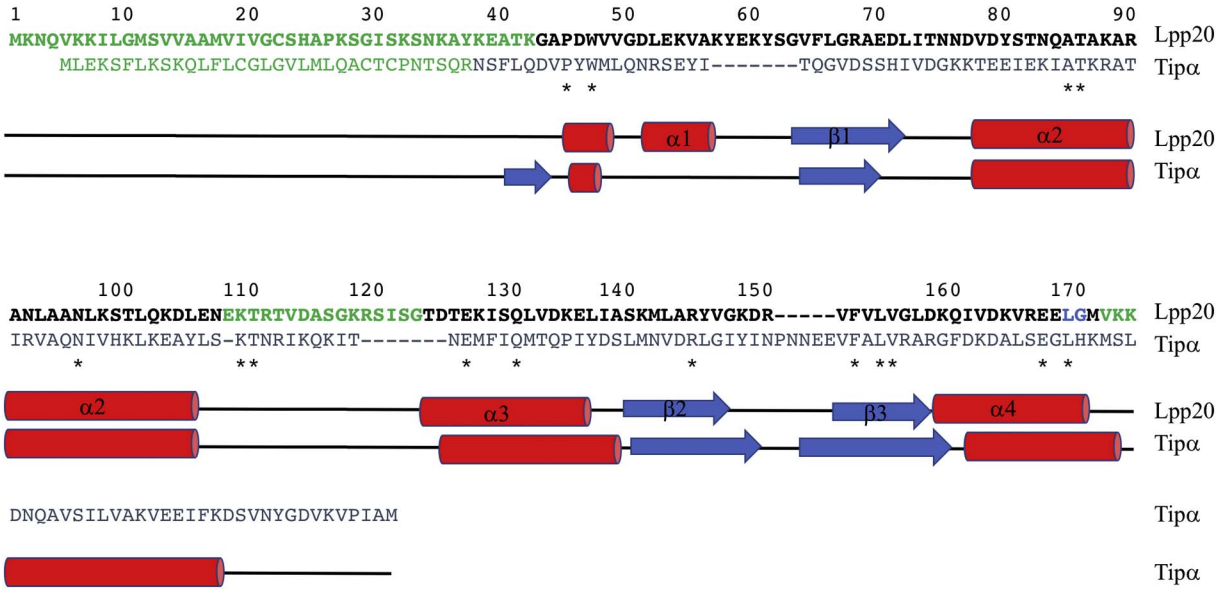

Fig. 1. Structural alignment of the amino acid sequence of Lpp20 from *H. pylori* with that of Tipα from the same bacterium [41–43]. Portions in green cannot be seen in the electron density map or were absent from the construct. Stars indicate amino acid identical in the two sequences. The position of secondary structure elements of both structures is shown below as red cylinders (α-helices) or blue arrows (β-strands).

3. Results

3.1. The three-dimensional structure of Lpp20 protein

The gene coding for HP1456, deprived of the first 60 nucleotides (corresponding to the 20 amino acids of the export signal sequence), has been cloned in *E. coli* cells and the protein expressed, purified and crystallized. The crystal structure was determined using the anomalous signal of the Seleno-methionine derivative.

In the electron density map (the full amino acid sequence of Lpp20 is reported in Fig. 1) visible residues start from Gly43 and extend to Asn107, and from Thr124 to Met172. The 21 residues at the N-terminus, the long loop from 108 to 125 and the last three residues are disordered and were not included in the model. The protein presents an elongated bent shape, made by a three-stranded anti-parallel β-sheet flanked by three α-helices on one side and a short α-helix on the other (Fig. 2A). The protein topology is α1-β1-α2-α3-β2-β3-α4. The two helices α2 and α3 are connected by a long flexible loop of 16 residues, not visible in the electron density map. Overall, two parts can be distinguished in the structure: a portion that includes the β-sheet, about half of long helix α2 and the N-terminus with helix α1; a second part consisting of a three-helix bundle, helices α3, α4 and the remaining half of helix α2. The two parts are bent with respect to each other, conferring a bent shape to the overall structure.

Four monomers (labeled A, B, C and D) of Lpp20 are present in the asymmetric unit (Fig. 2B). The four molecules are essentially identical, the root mean square deviation for the superposition of the Cα chain of monomers B, C and D to monomer A being 0.66 Å, 0.77 Å, and 0.78 Å. Only minor differences are visible at the end of helix α2 and at the beginning of helix α3, corresponding to the end and beginning of the long, disordered loop connecting them.

Monomers A - B and C - D are related to each other by a non-crystallographic local two-fold axis. The C - D interaction involves part of the surface of the long α2 and of α3 helices, whilst A and B monomers are in contact through the two helices α4. An analysis with server PISA did not detect enough specific interactions between monomers in the crystal, suggesting that the dimer present in the crystal is not the physiological one. A gel filtration analysis of the protein solution showed the presence of monomeric and dimeric species (Fig. S1A) and a SDS-PAGE in the presence or absence of 50 mM DTT showed that

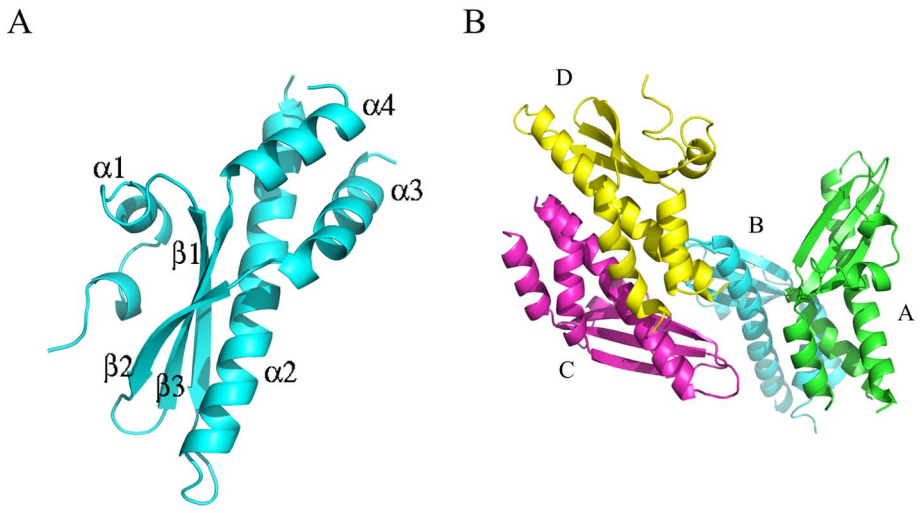

Fig. 2. Cartoon view of Lpp20 structure. A) Cartoon view of a monomer of Lpp20 with secondary structure elements labeled. B) Cartoon view of the four monomers of Lpp20 present in the asymmetric unit of the crystals. Monomers are represented in different colors and labeled as A, B, C and D.

dimerization is dependent on a disulfide bridge, mediated by Cys22 (Fig. S1B).

3.2. Identification of T and B epitopes on the Lpp20 structure

Two $CD4^+$ T cells and one B cells epitopes of Lpp20 were predicted, the corresponding peptides synthetized and tested in mice [15,16]. The positions of the three epitopes in the three-dimensional structure are shown in Fig. S2, where a general scheme of Lpp20 includes the parts of the protein not visible in the crystal structure. The protein is anchored to a membrane through the lipid, bound to the N-terminal Cys22. The chain comprising residues from 22 to 42 is flexible, and it represents the linker to the protein from the lipid that anchors it to the membrane. Since the linker is flexible and relatively long, this probably leaves a large flexibility to the protein orientation with respect to the membrane. Nevertheless, the most exposed part of Lpp20 is the loop connecting helices α2 and α3, which is fully flexible. The other two epitopes are quite long and only partially exposed, suggesting that perhaps the interacting portion of each of them is possibly shorter.

3.3. Analysis of the interactions of Lpp20 with other secreted proteins

STRING (http://string-db.org/cgi), a database that lists all the possible protein-protein interactions, considering direct (physical) and indirect (functional) associations, suggested possible interaction partners for Lpp20 (Fig. S3A). In particular, HP1454, HP1455 and HP1457, which are all located in the same operon of Lpp20. In addition, there are minor evidence supporting an interaction with TenA (HP1287, a member of the thiamine salvage pathway [36]), with the vacuolating cytotoxin VacA [37], and with Hp0224, predicted to be a peptide methionine sulfoxide reductase. Lpp20 operon includes four genes, from *hp1454* to *hp1457* [38]. HP1454 [27] is a secreted protein found in vesicles along with Lpp20 and HP1457 [39]. HP1457 is also predicted to be a lipoprotein present in the extracellular fraction [22] and up-regulated in acidic conditions [17].

We checked the interactions *in vitro* among these four proteins by mixing untagged Lpp20 together with each of the three other proteins, all containing a His-tag at the N-terminus, and eluting them from a nickel-affinity column. Before starting with the experiment, we ruled out any nonspecific binding of Lpp20 to the column (Fig. S3B). As shown in Fig. S3C, Lpp20 co-eluted with HP1457 but not with HP1454 and HP1455 (data not shown). Unfortunately, it is not possible to determine the molar ratio of this interaction, since the elution with imidazole removes from the column both the complex of the two proteins and HP1457 alone, not bound to Lpp20. This aspect deserves further investigation, including attempts to crystallize the complex Lpp20-HP1457.

3.4. Structural similarity of Lpp20 with Tipα

Taking advantage of the server DALI (http://ekhidna.biocenter.helsinki.fi/dali_server), we revealed that the three-dimensional structures of Lpp20 is similar to that of the TNF-α inducing protein (Tipα) [40], [41–43]. A superposition of the Cα chain trace of Lpp20 to Tipα is shown in Fig. 3. The r.m.s.d. between the two chains is 3.3 Å, and the topology of the two proteins is quite similar: they differ only for the presence of an additional, short α-helix at the N-terminus in Lpp20 and of an additional α-helix at the C-terminus in Tip-α. The qualitative electrostatic surface of both proteins, indicating a qualitative similarity, with a more charged face on one side and a more hydrophobic one on the other, is shown in Fig. S4.

Another intriguing similarity is found with the domain I of HP1454 [27], another protein of the same operon. Domain I includes a three-stranded β and a long α-helix that superimpose quite well to Lpp20 (r.m.s.d. 3.3 Å).

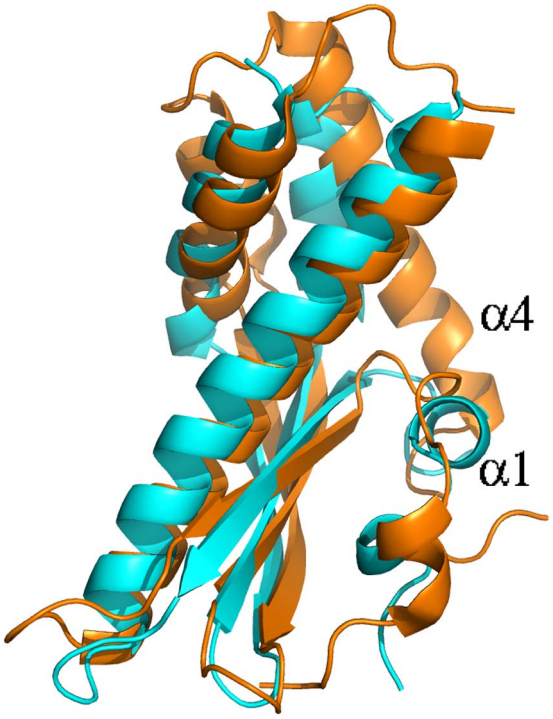

Fig. 3. Superposition of Cα chain trace of Lpp20 (cyan) to Tipα (orange; PDB ID code 2WCQ). α1 and α4 indicate the two α-helices present in Lpp20 and Tipα respectively, and absent in the other protein.

3.5. Lpp20 stimulates the migration and proliferation of gastric cancer cells

The high structural similarity between Lpp20 and Tipα and the fact that both proteins are secreted, suggested the possibility that they shared the same function in terms of pathogenicity. Therefore, we started by exploring the ability of Lpp20 in promoting the epithelial-mesenchymal transition (EMT), by evaluating its effects on cell migration and proliferation. For this purpose, we used the AGS cell line, that are non-metastatic gastric cancer cells from a poorly differentiated gastric adenocarcinoma [44].

The role of Lpp20 in cell migration was assessed by different approaches: Transwell migration assay, Scratch assay and filopodia formation. Fig. 4 shows that the exposure of AGS cells to wild-type Lpp20 was accompanied by a significant cell migration that was not recapitulated upon the application of the mutant form of Lpp20 (Lpp20C22A), unable to form dimers, thus supporting the notion that Lpp20 must be in its dimeric form to operate (Fig. S1A). The Scratch assay confirmed these results; as shown in Fig. 4A, the speed of wound repair was higher when AGS cells were treated with Lpp20 compared to those treated with Lpp20C22A or untreated. Finally, we evaluated filopodia formation in AGS cells induced by Lpp20. Filopodia are thin, actin-rich plasma-membrane protrusions that function as antennae for cells to probe their environment. They have an important role in cell migration. Actin filaments were stained with TRITC-conjugated phalloidin upon a 24 h-incubation with the proteins. We found that Lpp20 induced the formation of actin containing filaments around AGS cell surface, while the treatment with Lpp20C22A did not (Fig. 5). We believe that the observed phenotype might be associated with the Lpp20-induced migration of gastric cancer cells.

In parallel, we found that Lpp20 increased the proliferation rate in AGS cells (Fig. 6). Indeed, 5-(and 6-)carboxyfluorescein diacetate, succinimidyl ester probe (CFDA-SE) fluorescence intensity decreased after a 24 h-treatment with the wild type protein, whereas Lpp20C22A-treated cells showed the same proliferation rate recorded in untreated cells.

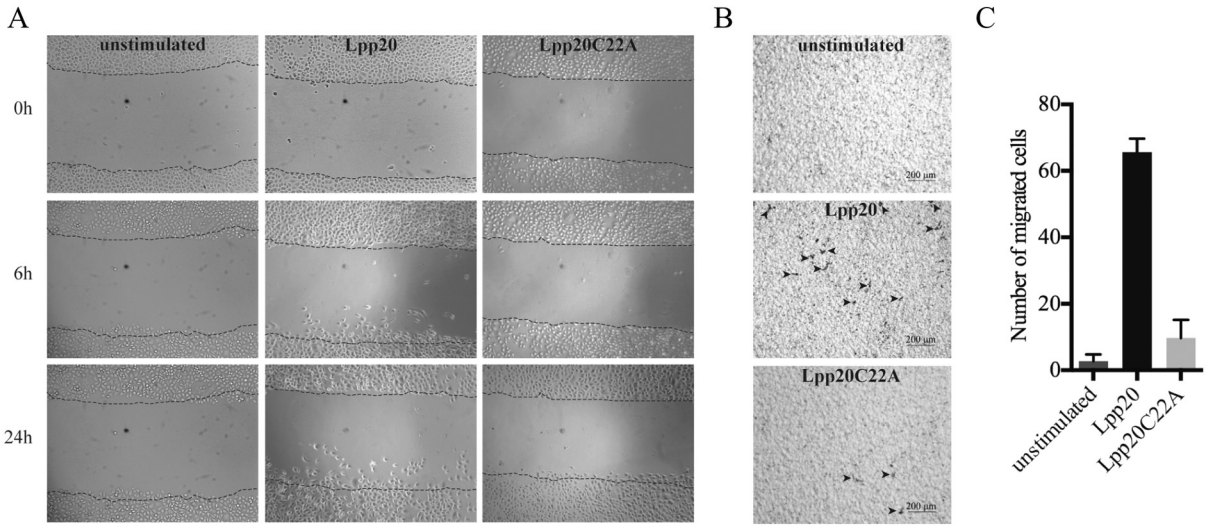

Fig. 4. Lpp20 stimulates AGS cell migration. Cell migration was evaluated after a 24 h incubation with Lpp20 or with Lpp20C22A (60 µg/ml) in serum-free RPMI (supplemented with 0.1% BSA). Cells incubated in medium alone, were considered as control (unstimulated). A) Cells were seeded in a 6-well plate and scratches were created once cells reached confluence. Cells were treated with Lpp20, Lpp20C22A or left untreated. At time zero and after 6 and 24 h, wound closures were photographed under a microscope (150 × magnification). Dotted lines delimitate the edge of the confluent monolayers. Representative wound closure images from three experiments are shown. B) A representative image of three experiments (80 × magnification) of Transwell migration is shown for each group. Only a portion of the membrane is shown. Arrow-heads point out migrated cells. C) Migration was expressed as the number of migrated cells counted in three different membranes.

3.6. Lpp20 reduces the expression of E-cadherin in gastric cancer cells

RT-PCR in Lpp20-treated AGS cells was performed to assess whether the expression of some proteins involved in EMT were modulated. We revealed that Lpp20, but not its mutant, induced a down regulation of the mRNA coding for E-cadherin in AGS cells (data not shown). EMT involving down-regulation of E-cadherin is thought to play a fundamental role during early steps of invasion and metastasis of carcinoma cells. However, AGS cells do not form a polarized epithelium and express the E-cadherin-catenin complex, critical for adherents junctions, only in an aberrant form [45]. In accordance, western blot analysis revealed a very low expression level of E-cadherin in AGS cells (data not shown); hence, we decided to confirm our results on MKN-28 cells, since these cells showed a similar behavior of AGS cells following

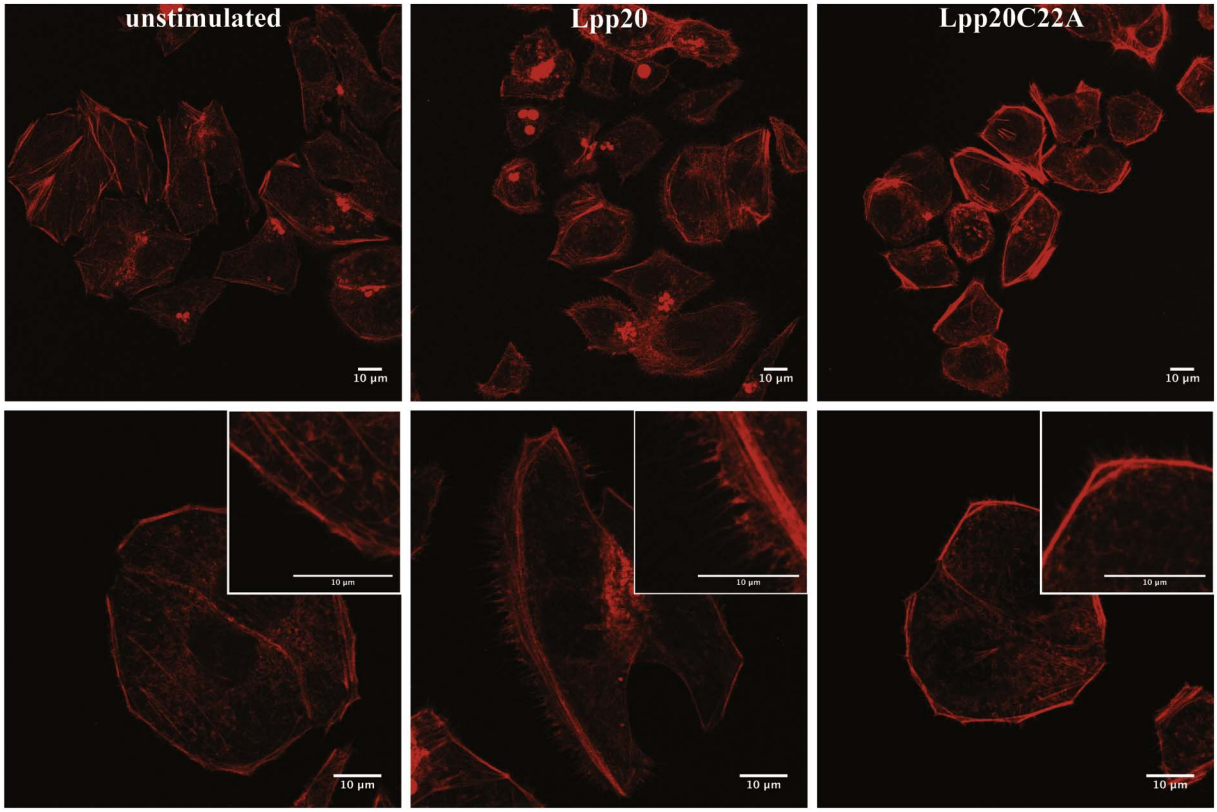

Fig. 5. Filopodia formation in AGS cells exposed to Lpp20 and Lpp20C22A. AGS cells were treated with Lpp20, Lpp20C22A or left untreated and then stained with TRITC-conjugated phalloidin. Representative images from three experiments performed with different cell preparation are shown.

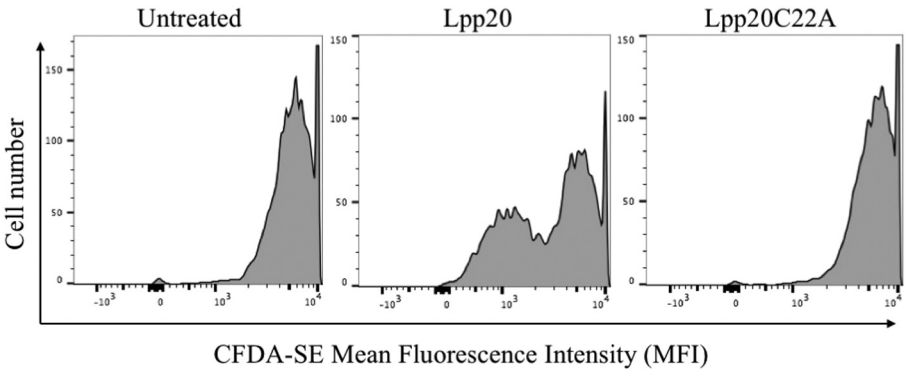

Fig. 6. Proliferation of AGS cells exposed to Lpp20 and Lpp20C22A. Cells were labeled with CFDA-SE and incubated 24 h with Lpp20, Lpp20C22A or left untreated in RPMI, 0.1% BSA medium. Cells were harvested, washed, re-suspended in PBS, and analyzed by flow cytometry. Representative histograms from two independent experiments are reported.

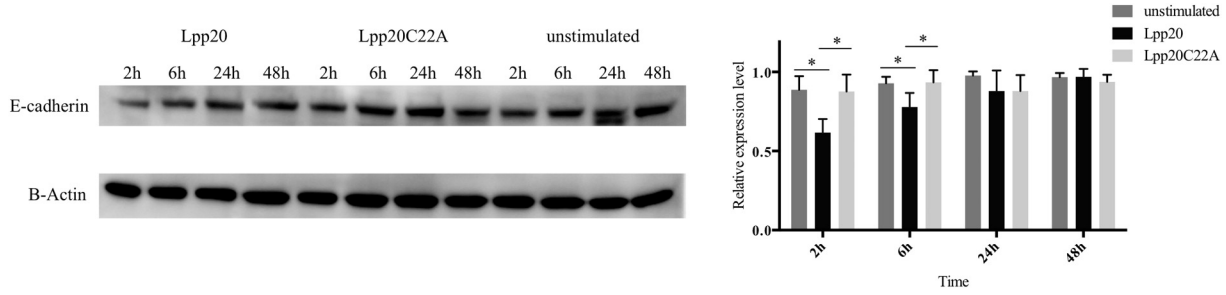

Fig. 7. Effect of Lpp20 on E-cadherin expression. Western blot analysis of E-cadherin using whole cell lysates of MKN-28 cells treated for 2, 6, 24 and 48 h with Lpp20 or Lpp20C22A 60 μg/ml or left untreated. Bar diagram shows the change in E-cadherin protein expression normalized to that of β-actin. The highest value was taken as reference and set as 1 A.U. Data are presented as the mean ± SD of four independent experiments. $*p < 0.05$.

the exposure to Lpp20 and Lpp20C22A (Supplementary Figs. S5 and S6). Treatment of MKN-28 cells with Lpp20 decreased the expression of E-cadherin (Fig. 7), with a maximal effect within 2 h of stimulation before returning to the basal level. In contrast, the mutant form of Lpp20C22A did not affect E-cadherin expression. These results corroborate the idea that Lpp20 dimer could act as an inducer of EMT in gastric cancers.

4. Discussion

Lpp20 protein is an important immunogenic factor of *H. pylori*, but its physiological function has not been analyzed in depth. The protein is bound to the outer membrane of the bacterium, but it is also secreted inside vesicles [39]. The physiological function of all the proteins coded by the operon including genes from *hp1454* to *hp1457* is unknown, but it is known that at least three of them, i.e. HP1454, HP1456 (Lpp20) and HP1457, are secreted together inside vesicles. In addition, here we report that Lpp20 and HP1457 proteins interact *in vitro*. Deciphering the three-dimensional structure of Lpp20 revealed that it is very similar to that of Tipα. Both Tipα and Lpp20 form dimers, mediated by a cysteine located in a similar position in the sequence, at the N-terminus. Lpp20 and Tipα also contain a LVGCS motif (with a serine as the +2 amino acid) at the C-terminal end of their signal sequences, which is characteristic for lipoprotein precursors [20]. Lpp20 is considered as an outer membrane-associated lipoprotein [46], while Tipα is rather loosely connected to the inner membrane and potentially secreted during infection [47,48]. The released lipoproteins are potential factors playing a role in bacterial pathogenesis, mainly due to the stimulation of eukaryotic cells throughout Toll-like receptors (TLR2). Moreover, both proteins are highly immunogenic.

Tipα is a carcinogenic and inflammatory factor. It consists of 172 amino acids and its homo-dimer is a strong TNF-α inducer, whereas del-Tipα, a deletion mutant lacking the N-terminus, is an inactive monomer [23] [24]. Secreted Tipα is incorporated into gastric cancer cells by directly binding on the cell surface to nucleolin. The binding triggers the activation of the transcription factor NF-κB and induces the expression of TNF-α and chemokine genes. Although the down-regulation of E-cadherin was not shown in cells, Tipα induces the expression of vimentin and morphological changes in human gastric cancer cells, thus recalling the epithelial–mesenchymal transition (EMT) process. However, it is not known yet which particular molecule of *H. pylori* promotes EMT in gastric cancer cells [48,49].

We demonstrated *in vitro* that Lpp20 induces E-cadherin down-regulation in gastric cancer cells, but it also promotes cell migration, cell proliferation, and the formation of filopodia.

These effects were limited or absent using Lpp20C22A, a Lpp20 mutant that has lost the possibility to form a homo-dimer through the formation of a disulfide bridge with cysteine in position 22. These results have two important implications: i) they reveal that the Cys22, which is the N-terminal residue after the removal of the signal sequence required to export the protein to the periplasm, is essential for protein dimerization and that the homo-dimer of Lpp20 is the active form of the protein; ii) they permit to rule out that the effects we observed on gastric cancer cells with Lpp20 were due to the presence of a contaminant in the preparation, such as the lipopolysaccharide of *E. coli*, being the latter adopted to express the recombinant protein.

The results obtained, in addition to the rationalization of the immunogenic behavior of the protein, suggest important clues about the physiology of Lpp20. In a way similar to its structural homologue Tipα, a recognized carcinogenic factor of *H. pylori*, it induces EMT in human gastric cancer cell lines. In doing so, it may stimulate tumor progression. Our evidence permits to speculate that Tipα and Lpp20 might work in parallel or in synergy, possibly triggering different pathways, in promoting the EMT, thus favoring the metastatic process of the gastric cancer. Therefore, we suggest to include Lpp20 in the list of virulence factors of *H. pylori*.

Transparency document

The Transparency document associated with this article can be found, in the online version.

Accession number PDB ID: 5OK8

Acknowledgments

We thank Valentina Loconte for the clone of HP1457. The staff of beamline PXIII of Swiss Light Source (SLS), Villigen (Switzerland), and of ID23-2 of European Synchrotron Radiation Facility (ESRF), Grenoble (France) for technical assistance during data collection.

Funding

This work was supported by the University of Padua and by PRIN 2010–2011 (MIUR) "*Unraveling structural and functional determinants behind Helicobacter pylori pathogenesis and persistence*". Support for data collection was also received from the European Community's Seventh Framework Program (FP7/2007–2013) under grant agreement n. 283,570 (BioStruct-X).

Appendix A. Supplementary data

Supplementary data to this article can be found online at https://doi.org/10.1016/j.bbagen.2017.09.017.

References

[1] C. Montecucco, R. Rappuoli, Living dangerously: how Helicobacter pylori survives in the human stomach, Nat. Rev. Mol. Cell Biol. 2 (2001) 457–466, http://dx.doi.org/10.1038/35073084.
[2] D.Y. Graham, History of Helicobacter pylori, duodenal ulcer, gastric ulcer and gastric cancer, World J. Gastroenterol. 20 (2014) 5191–5204, http://dx.doi.org/10.3748/wjg.v20.i18.5191.
[3] B.R. Bloom, Vaccines for the Third World, Nature 342 (1989) 115–120, http://dx.doi.org/10.1038/342115a0.
[4] R.L. Ferrero, J.-M. Thiberge, M. Huerre, A. Labigne, Recombinant antigens prepared from the urease subunits of Helicobacter spp.: evidence of protection in a mouse model of gastric infection, Infect. Immun. 62 (1994) 4981–4989.
[5] R.L. Ferrero, J.-M. Thiberge, I. Kansau, N. Wuscher, M. Huerre, A. Labigne, The GroES homolog of Helicobacter pylori confers protective immunity against mucosal infection in mice, Proc. Natl. Acad. Sci. U. S. A. 92 (1995) 6499–6503.
[6] M. Marchetti, B. Arico, D. Burroni, N. Figura, R. Rappuoli, P. Ghiara, Development of a mouse model of Helicobacter pylori infection that mimics human disease, Science 267 (1995) 1655–1658.
[7] F.J. Radcliff, S.L. Hazell, T. Kolesnikow, C. Doidge, A. Lee, Catalase, a novel antigen for Helicobacter pylori vaccination, Infect. Immun. 65 (1997) 4668–4674.
[8] B. Satin, G. Del Giudice, V. Della Bianca, S. Dusi, C. Laudanna, F. Tonello, et al., The neutrophil-activating protein (HP-NAP) of Helicobacter pylori is a protective antigen and a major virulence factor, J. Exp. Med. 191 (2000) 1467–1476.
[9] G. Del Giudice, A. Covacci, J.L. Telford, C. Montecucco, R. Rappuoli, The design of vaccines against Helicobacter pylori and their development, Annu. Rev. Immunol. 19 (2001) 523–563, http://dx.doi.org/10.1146/annurev.immunol.19.1.523.
[10] B. Sun, Z.-S. Li, Z.-X. Tu, G.-M. Xu, Y.-Q. Du, Construction of an oral recombinant DNA vaccine from H pylori neutrophil activating protein and its immunogenicity, World J. Gastroenterol. 12 (2006) 7042–7046, http://dx.doi.org/10.3748/wjg.v12.i43.7042.
[11] G. Zanotti, E. Papinutto, W. Dundon, R. Battistutta, M. Seveso, G. Giudice, et al., Structure of the neutrophil-activating protein from Helicobacter pylori, J. Mol. Biol. 323 (2002) 125–130.
[12] D. Hocking, E. Webb, F. Radcliff, L. Rothel, S. Taylor, G. Pinczower, et al., Isolation of recombinant protective Helicobacter pylori antigens, Infect. Immun. 67 (1999) 4713–4719.
[13] M. Zeng, X.-H. Mao, J.-X. Li, W.-D. Tong, B. Wang, Y.-J. Zhang, et al., Efficacy, safety, and immunogenicity of an oral recombinant Helicobacter pylori vaccine in children in China: a randomised, double-blind, placebo-controlled, phase 3 trial, Lancet 386 (2015) 1457–1464, http://dx.doi.org/10.1016/S0140-6736(15)60310-5.
[14] J. Keenan, J. Oliaro, N. Domigan, H. Potter, G. Aitken, R. Allardyce, et al., Immune response to an 18-kilodalton outer membrane antigen identifies lipoprotein 20 as a Helicobacter pylori vaccine candidate, Infect. Immun. 68 (2000) 3337–3343.
[15] W. Yu, Y. Zhang, J. Jing, Z. Liu, Construction of Helicobacter pylori Lpp20-IL2 DNA vaccine and evaluation of its immunocompetence in C57BL/6 mice, Wei Sheng Wu Xue Bao 50 (2010) 554–559.
[16] Y. Li, Z. Chen, J. Ye, L. Ning, J. Luo, L. Zhang, et al., Antibody production and Th1-biased response induced by an epitope vaccine composed of cholera toxin B unit and helicobacter pylori Lpp20 epitopes, Helicobacter 21 (2016) 234–248, http://dx.doi.org/10.1111/hel.12268.
[17] Y. Wen, E.A. Marcus, U. Matrubutham, M.A. Gleeson, D.R. Scott, G. Sachs, Acid-adaptive genes of Helicobacter pylori, Infect. Immun. 71 (2003) 5921.
[18] D.S. Merrell, L.J. Thompson, C.C. Kim, H. Mitchell, L.S. Tompkins, A. Lee, et al., Growth phase-dependent response of Helicobacter pylori to iron starvation, Infect. Immun. 71 (2003) 6510.
[19] F.D. Ernst, S. Bereswill, B. Waidner, J. Stoof, U. Mäder, J.G. Kusters, et al., Transcriptional profiling of Helicobacter pylori Fur- and iron-regulated gene expression, Microbiology, 151 2005, pp. 533–546 (Reading, Engl.).
[20] M. Kostrzynska, P.W. O'Toole, D.E. Taylor, T.J. Trust, Molecular characterization of a conserved 20-kilodalton membrane-associated lipoprotein antigen of Helicobacter pylori, J. Bacteriol. 176 (1994) 5938–5948.
[21] N.R. Salama, B. Shepherd, S. Falkow, Global transposon mutagenesis and essential gene analysis of Helicobacter pylori, J. Bacteriol. 186 (2004) 7926–7935, http://dx.doi.org/10.1128/JB.186.23.7926-7935.2004.
[22] T.G. Smith, J.-M. Lim, M.V. Weinberg, L. Wells, T.R. Hoover, Direct analysis of the extracellular proteome from two strains of Helicobacter pylori, Proteomics 7 (2007) 2240–2245, http://dx.doi.org/10.1002/pmic.200600875.
[23] M. Suganuma, K. Yamaguchi, Y. Ono, H. Matsumoto, T. Hayashi, T. Ogawa, et al., TNF-alpha-inducing protein, a carcinogenic factor secreted from H. pylori, enters gastric cancer cells, Int J Cancer. 123 (2008) 117–122, http://dx.doi.org/10.1002/ijc.23484.
[24] M. Suganuma, T. Watanabe, K. Yamaguchi, A. Takahashi, H. Fujiki, Human gastric cancer development with TNF-α-inducing protein secreted from Helicobacter pylori, Cancer Lett. 322 (2012) 133–138, http://dx.doi.org/10.1016/j.canlet.2012.03.027.
[25] S. Lamouille, J. Xu, R. Derynck, Molecular mechanisms of epithelial-mesenchymal transition, Nat. Rev. Mol. Cell Biol. 15 (2014) 178–196, http://dx.doi.org/10.1038/nrm3758.
[26] T. Watanabe, A. Takahashi, K. Suzuki, M. Kurusu-Kanno, K. Yamaguchi, H. Fujiki, et al., Epithelial-mesenchymal transition in human gastric cancer cell lines induced by TNF-α-inducing protein of Helicobacter pylori, Int. J. Cancer 134 (2014) 2373–2382, http://dx.doi.org/10.1002/ijc.28582.
[27] S. Quarantini, L. Cendron, G. Zanotti, Crystal structure of the secreted protein HP1454 from the human pathogen Helicobacter pylori, Proteins 82 (2014) 2868–2873, http://dx.doi.org/10.1002/prot.24608.
[28] W. Kabsch, Integration, scaling, space-group assignment and post-refinement, Acta Crystallogr. D Biol. Crystallogr. 66 (2010) 133–144, http://dx.doi.org/10.1107/S0907444909047374.
[29] P. Evans, Scaling and assessment of data quality, Acta Crystallogr. D Biol. Crystallogr. 62 (2006) 72–82, http://dx.doi.org/10.1107/S0907444905036693.
[30] M.D. Winn, C.C. Ballard, K.D. Cowtan, E.J. Dodson, P. Emsley, P.R. Evans, et al., Overview of the CCP4 suite and current developments, Acta Crystallogr. D Biol. Crystallogr. 67 (2011) 235–242, http://dx.doi.org/10.1107/S0907444910045749.
[31] T.C. Terwilliger, P.D. Adams, R.J. Read, A.J. Mccoy, N.W. Moriarty, R.W. Grosse-Kunstleve, et al., Decision-making in structure solution using Bayesian estimates of map quality: the PHENIX AutoSol wizard, Acta Crystallogr. D Biol. Crystallogr. 65 (2009) 582–601, http://dx.doi.org/10.1107/S0907444909012098.
[32] K. Cowtan, The Buccaneer software for automated model building. 1. Tracing protein chains, Acta Crystallogr. D Biol. Crystallogr. 62 (2006) 1002–1011, http://dx.doi.org/10.1107/S0907444906022116.
[33] P.D. Adams, P.V. Afonine, G. Bunkóczi, V.B. Chen, I.W. Davis, N. Echols, et al., PHENIX: a comprehensive Python-based system for macromolecular structure solution, Acta Crystallogr. D Biol. Crystallogr. 66 (2010) 213–221, http://dx.doi.org/10.1107/S0907444909052925.
[34] P. Emsley, B. Lohkamp, W.G. Scott, K. Cowtan, Features and development of Coot, Acta Crystallogr. D Biol. Crystallogr. 66 (2010) 486–501, http://dx.doi.org/10.1107/S0907444910007493.
[35] A.E. Karnoub, A.B. Dash, A.P. Vo, A. Sullivan, M.W. Brooks, G.W. Bell, et al., Mesenchymal stem cells within tumour stroma promote breast cancer metastasis, Nature 449 (2007) 557–563, http://dx.doi.org/10.1038/nature06188.
[36] N. Barison, L. Cendron, A. Trento, A. Angelini, G. Zanotti, Structural and mutational analysis of TenA protein (HP1287) from the Helicobacter pylori thiamin salvage pathway - evidence of a different substrate specificity, FEBS J. 276 (2009) 6227–6235, http://dx.doi.org/10.1111/j.1742-4658.2009.07326.x.
[37] R.M. Delahay, M. Rugge, Pathogenesis of Helicobacter pylori infection, Helicobacter 17 (Suppl. 1) (2012) 9–15, http://dx.doi.org/10.1111/j.1523-5378.2012.00976.x.
[38] C.M. Sharma, S. Hoffmann, F. Darfeuille, J. Reignier, S. Findeiß, A. Sittka, et al., The primary transcriptome of the major human pathogen Helicobacter pylori, Nature 464 (2010) 250–255, http://dx.doi.org/10.1038/nature08756.
[39] A. Olofsson, A. Vallstrom, K. Petzold, N. Tegtmeyer, J. Schleucher, S. Carlsson, et al., Biochemical and functional characterization of Helicobacter pylori vesicles, Mol. Microbiol. 77 (2010) 1539–1555, http://dx.doi.org/10.1111/j.1365-2958.2010.07307.x.
[40] H. Tsuge, T. Tsurumura, H. Utsunomiya, D. Kise, T. Kuzuhara, T. Watanabe, et al., Structural basis for the Helicobacter pylori-carcinogenic TNF-alpha-inducing protein, Biochem. Biophys. Res. Commun. 388 (2009) 193–198, http://dx.doi.org/10.1016/j.bbrc.2009.07.121.
[41] T. Tosi, G. Cioci, K. Jouravleva, C. Dian, L. Terradot, Structures of the tumor necrosis factor alpha inducing protein Tip alpha: a novel virulence factor from Helicobacter pylori, FEBS Lett. 583 (2009) 1581–1585, http://dx.doi.org/10.1016/j.febslet.2009.04.033.
[42] J.Y. Jang, H.-J. Yoon, J.Y. Yoon, H.S. Kim, S.J. Lee, K.H. Kim, et al., Crystal structure of the TNF-alpha-Inducing protein (Tipalpha) from Helicobacter pylori: insights into its DNA-binding activity, J. Mol. Biol. 392 (2009) 191–197, http://dx.doi.org/10.1016/j.jmb.2009.07.010.
[43] M. Gao, D. Li, Y. Hu, Y. Zhang, Q. Zou, D.-C. Wang, Crystal structure of TNF-α-inducing protein from Helicobacter pylori in active form reveals the intrinsic molecular flexibility for unique DNA-binding, PLoS One 7 (2012) e41871, , http://dx.doi.org/10.1371/journal.pone.0041871.
[44] S.C. Barranco, C.M. Townsend, C. Casartelli, B.G. Macik, N.L. Burger, W.R. Boerwinkle, et al., Establishment and characterization of an *in vitro* model

system for human adenocarcinoma of the stomach, Cancer Res. 43 (1983) 1703–1709.
[45] A.U. Jawhari, M. Noda, M.J. Farthing, M. Pignatelli, Abnormal expression and function of the E-cadherin-catenin complex in gastric carcinoma cell lines, Br. J. Cancer 80 (1999) 322–330, http://dx.doi.org/10.1038/sj.bjc.6690358.
[46] B.J. Voss, J.A. Gaddy, W.H. McDonald, T.L. Cover, Analysis of surface-exposed outer membrane proteins in Helicobacter pylori, J. Bacteriol. 196 (2014) 2455–2471, http://dx.doi.org/10.1128/JB.01768-14.
[47] R. Godlewska, M. Pawlowski, A. Dzwonek, M. Mikula, J. Ostrowski, N. Drela, et al., Tip-alpha (hp0596 gene product) is a highly immunogenic Helicobacter pylori protein involved in colonization of mouse gastric mucosa, Curr. Microbiol. 56 (2008) 279–286, http://dx.doi.org/10.1007/s00284-007-9083-7.
[48] T. Watanabe, H. Tsuge, T. Imagawa, D. Kise, K. Hirano, M. Beppu, et al., Nucleolin as cell surface receptor for tumor necrosis factor-alpha inducing protein: a carcinogenic factor of Helicobacter pylori, J. Cancer Res. Clin. Oncol. 136 (2010) 911–921, http://dx.doi.org/10.1007/s00432-009-0733-y.
[49] M.A. Huber, H. Beug, T. Wirth, Epithelial-mesenchymal transition: NF-kappaB takes center stage, Cell Cycle 3 (2004) 1477–1480, http://dx.doi.org/10.4161/cc.3.12.1280.